

Comprehensive structural classification of ligand binding motifs in proteins

Akira R. Kinjo^{a,*} and Haruki Nakamura^a

^a*Institute for Protein Research, Osaka University, 3-2 Yamadaoka, Suita, Osaka 565-0871, Japan*

Abstract

Comprehensive knowledge of protein-ligand interactions should provide a useful basis for annotating protein functions, studying protein evolution, engineering enzymatic activity, and designing drugs. To investigate the diversity and universality of ligand binding sites in protein structures, we conducted the all-against-all atomic-level structural comparison of over 180,000 ligand binding sites found in all the known structures in the Protein Data Bank by using a recently developed database search and alignment algorithm. By applying a hybrid top-down-bottom-up clustering analysis to the comparison results, we determined approximately 3000 well-defined structural motifs of ligand binding sites. Apart from a handful of exceptions, most structural motifs were found to be confined within single families or superfamilies, and to be associated with particular ligands. Furthermore, we analyzed the components of the similarity network and enumerated more than 4000 pairs of ligand binding sites that were shared across different protein folds.

Introduction Most proteins function by interacting with other molecules. Therefore, the knowledge of interactions between proteins and their ligands is central to our understanding of protein functions. However, simply enumerating the interactions of individual proteins with individual ligands, which is now indeed possible owing to the massive production of experimentally determined protein structures, would only serve to increase the amount of data, not necessarily our knowledge or understanding, of protein functions. What is needed is a classification of general patterns of interactions. Otherwise, it would be difficult to apply the wealth of information to elucidate the evolutionary history of protein functions (Andreeva & Murzin, 2006; Goldstein, 2008), to engineer enzymatic activity (Gutteridge & Thornton, 2005), or to develop new drugs (Rognan, 2007).

In order to classify protein-ligand interactions and to extract general patterns from the classification, it is a prerequisite to compare the ligand binding sites of different proteins. There are already a number of methods to compare the atomic structures or other structural features of functional sites of proteins (see reviews, Jones & Thornton, 2004; Lee *et al.*, 2007).

Applications of these methods lead to the discoveries of ligand binding site structures shared by many proteins

of different folds (Kobayashi & Go, 1997; Kinoshita *et al.*, 1999; Stark & Russell, 2003; Brakoulias & Jackson, 2004; Shulman-Peleg *et al.*, 2004; Gold & Jackson, 2006). Gold & Jackson (2006) conducted an all-against-all comparison of 33,168 binding sites, the results of which have been compiled into the SitesBase database. They have described several unexpected similarities across different protein folds and applied their method to the annotation of unclassified proteins. More recently, Minai *et al.* (2008) compared all pairs of 48,347 potential ligand binding sites in 9708 representative protein chains, and demonstrated the applicability of ligand binding site comparison to drug discovery.

To date, however, no method has been applied to the exhaustive all-against-all comparison of all ligand binding sites found in the Protein Data Bank (PDB) (Berman *et al.*, 2007), presumably because these methods were not efficient enough to handle the huge amount of data in the current PDB, or because it was assumed that the redundancy (in terms of sequence homology) or some “trivial” ligands (such as sulfate ions) in the PDB did not present any interesting findings. As of June, 2008, the PDB contains over 51,000 entries with more than 180,000 ligand binding sites excluding water molecules, and hence naively comparing all the pairs of this many binding sites ($> 3 \times 10^{10}$ pairs) is indeed a formidable task. Nevertheless, multiple structures of many proteins that have been solved with a variety of ligands (e.g., inhibitors for enzymes) could provide a great opportunity for analyzing

* Corresponding author

Email address: akinjo@protein.osaka-u.ac.jp (Akira R. Kinjo).

the diversity of binding modes, and some apparently trivial ligands are often used by crystallographers to infer the functional sites from the “apo” structure. In other words, the diversity of these apparently redundant data is too precious a source of information to be ignored.

To handle this huge amount data, we have recently developed the GIRAF (Geometric Indexing with Refined Alignment Finder) method (Kinjo & Nakamura, 2007). By combining ideas from geometric hashing (Wolfson & Rigoutsos, 1997) and relational database searching (Garcia-Molina *et al.*, 2002), this method can efficiently find structurally and chemically similar local protein structures in a database and produce alignments at atomic resolution independent of sequence homology, sequence order, or protein fold. In this method, we first compile a database of ligand binding sites into an ordinary relational database management system, and create an index based on the geometric features with surrounding atomic environments. Owing to the index, potentially similar ligand binding sites can be efficiently retrieved and unlikely hits are safely ignored. For each of the potential hits found, the refined atom-atom alignment is obtained by iterative applications of bipartite graph matching and optimal superposition. In this study, we have further improved the original GIRAF method so that one-against-all comparison takes effectively one second, and applied it to the first all-against-all comparison of all ligand binding sites in the PDB.

In order to extract recurring patterns in ligand binding sites, we then classified the ligand binding sites based on the results of the all-against-all comparison, and defined structural motifs. So far, such structural motifs have been determined either manually (Porter *et al.*, 2004) or automatically (Wangikar *et al.*, 2003; Polacco & Babbitt, 2006). Given the huge amount of data, manual curation of all potential motifs is not feasible, and previously developed automatic methods are computationally too intensive (Wangikar *et al.*, 2003) or limited in scope (e.g., being based on sequence alignment (Polacco & Babbitt, 2006)). Therefore, we first applied divisive (top-down) hierarchical clustering to obtain single-linkage clusters from the similarity network of ligand binding sites which can be readily obtained from the result of the all-against-all comparison. Based on the hierarchy of the single-linkage clusters, agglomerative (bottom-up) complete-linkage clustering is then applied. Thus obtained complete-linkage clusters are shown to be well-defined structural motifs, and are then subject to statistical characterization regarding their ligand specificity and protein folds.

Furthermore, based on the result of the all-against-all comparison, we study the structure of the similarity network of ligand binding sites, and enumerate interesting similarities shared across different folds. The list of clusters and the list of pairs of ligand binding sites not sharing the same fold are available on-line¹.

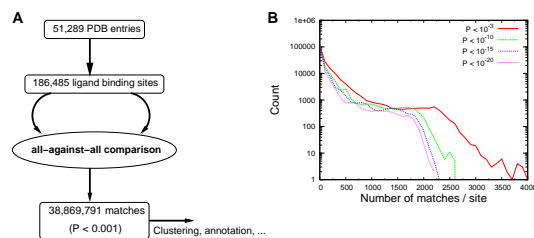


Fig. 1. Summary of experiment. **A**: Flow of the analysis. **B**: Histogram of the number of matches per ligand binding site.

Results

All-against-all comparison of ligand binding sites

Out of 51,289 entries in the Protein Data Bank (Berman *et al.*, 2007) as of June 13, 2008, all 186,485 ligand binding sites were extracted and compiled into a database. A ligand binding site is defined to be the set of protein atoms that are within 5Å from any of the corresponding ligand atoms. To define a ligand, we used the annotations in PDB’s canonical XML (extensible markup language) files (PDBML) (Westbrook *et al.*, 2005) because these annotations are more accurate than the HETATM record of the flat PDB files. Our definition of ligands includes not only small molecules, but also polymers such as polydeoxyribonucleotide (DNA), polyribonucleotide (RNA), polysaccharides, and polypeptides with less than 25 amino acid residues; water molecules and ligands consisting of more than 1000 atoms were excluded. We did not exclude “trivial” ligands such as sulfate (SO_4^{2-}), phosphate (PO_4^{3-}), and metal ions. We did not use a representative set of proteins based on sequence homology to reduce the data size.

In total, the all-against-all comparison yielded 38,869,791 matches with P-value < 0.001 with 208 matches per site on average (Fig. 1A). While 5014 sites found no hits other than themselves, 8369 sites found more than 1000 matches. When we limit the matches to more stringent P-value thresholds (10^{-10} , 10^{-15} , 10^{-20}), the long tail of the large number of matches rapidly disappears (Fig. 1B), indicating that many matches reflect partial and weak similarities between sites.

Relationship between similarities of protein sequences and ligand binding sites As noted above, the present data set is highly redundant in terms of sequence homology. If the similarity of ligand binding sites is sharply correlated with that of amino acid sequences, it would have been better to use sequence representatives. To justify the use of the redundant data set, we carried out an all-against-all

¹ <http://pdbjs6.pdbj.org/~akinjo/lbs/>

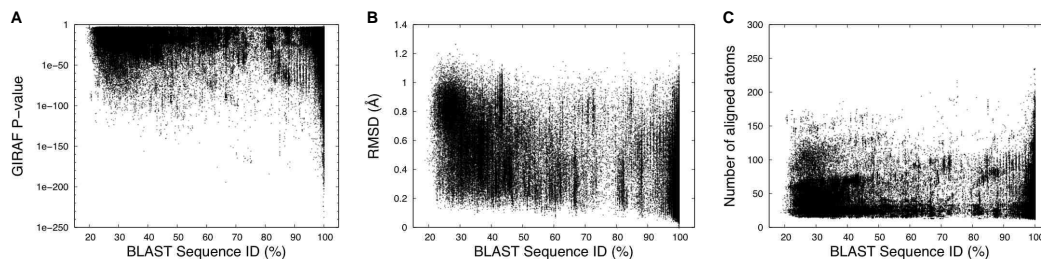


Fig. 2. Relationship between sequence similarity and ligand binding site similarity. **A**: Sequence identity of BLAST hits versus GIRAF P-values. **B**: Sequence identity of BLAST hits versus root-mean-square deviation of aligned ligand binding sites found by GIRAF. **C**: Sequence identity of BLAST hits versus the number of ligand binding site atoms aligned by GIRAF.

BLAST (Altschul *et al.*, 1997) search of all protein chains of the present data set, and checked the correlation between sequence identity and GIRAF P-value (Fig. 2A). It should be noted that a ligand binding site may reside at an interface of more than two protein subunits (chains), which complicates the notion of representative chains. Therefore, we defined sequence similarity between two PDB entries as the maximum sequence identity of all the possible pairs of chains from the two PDB entries.

While there was a significant but very weak negative correlation between the GIRAF P-value and percent sequence identity (Pearson’s correlation -0.14), there were many strikingly similar (GIRAF P-value $< 10^{-50}$) pairs of ligand binding sites with low ($< 30\%$) sequence identity, and there were also many weakly similar ligand binding sites (GIRAF P-value $> 10^{-20}$) at high ($> 90\%$) sequence identity region. This tendency was also confirmed by using more conventional measures of similarities. Although the root-mean-square deviation (RMSD) of aligned atoms exhibited a stronger negative correlation with the sequence identity (Fig. 2B; Pearson’s correlation -0.46), the range of scatter of RMSD was so large that it was not possible to distinguish the range of sequence identity from RMSD values and *vice versa*. In addition, the number of aligned atoms did not correlate with the sequence identity (Fig. 2C), indicating that the local structures of ligand binding sites can be strictly conserved among distantly related proteins. Visual inspection suggested a few possible reasons for the large deviation in the region of high sequence similarity. First, the binding sites do not necessarily overlap completely when different ligands are complexed with (almost) identical proteins. Second, many binding sites are flexible, yet they are able to bind the same ligand. Third, some ligands are flexible and can be bound as different conformers, which in turn causes structural changes of the binding site.

One of the rationales for an exhaustive all-against-all comparison is that some similarities between non-representative proteins would be ignored when only sequence representatives were used. For example, in the results of a comparison of potential ligand binding sites of 9708 sequence representative proteins conducted by Minai *et al.* (2008), the similarity between the ADP binding sites of human inositol (1,4,5)-triphosphate 3-kinase (PDB: 1W2D (Gonzalez *et al.*, 2004); SAICAR synthase-

like fold) and of *Archaeoglobus fulgidus* Rio2 kinase (PDB: 1ZAR (Laronde-Leblanc *et al.*, 2005); Protein kinase-like fold) was not detected although this match was found to have P-value of 8.1×10^{-17} (40 aligned atoms; RMSD 0.75Å) in the present result. Furthermore, equivalent matches were found in not all homologs of these two proteins. We note, however, that Minai *et al.* (2008) did find an equivalent similarity between the binding sites of these protein folds, but it was based on apo structures which were not treated here. Thus, the similarity not detected by Minai *et al.* is likely to be due to the use of representatives, but not due to the difference in sensitivity of their method and the present one.

We conclude that the similarity of sequences and that of ligand binding site structures are weakly correlated, but the correlation is not strong enough to infer the one from the other.

Defining structural motifs of ligand binding sites We have seen that sequence representatives are not suitable for studying the diversity of ligand binding sites. The use of the raw data of ligand binding sites for statistical analysis, however, would be problematic due to some over-represented and under-represented binding sites. Therefore, it is preferable to remove the redundancy based on the ligand binding similarity itself. Furthermore, a list of pairwise similarities is not sufficient for characterizing typical patterns of binding modes. Accordingly, we applied the hybrid top-down-bottom-up clustering method to obtain complete-linkage clusters based on P-value. In a complete-linkage cluster (hereafter referred to as ‘cluster’), any pair of its members are similar within the specified P-value threshold. As such, clusters may be regarded as precisely defined structural motifs of ligand binding sites, and hence we use the term ‘cluster’ and ‘structural motif’ (or simply ‘motif’) interchangeably when appropriate. Based on the analysis of similarity networks with varying thresholds (see below), we set the threshold to 10^{-15} in the following analysis.

It is immediately evident that there are a large number of small clusters and a small number of large clusters (Fig. 3A). Excluding 58,001 singletons (clusters with only one member), there were 20,224 clusters which accounted for

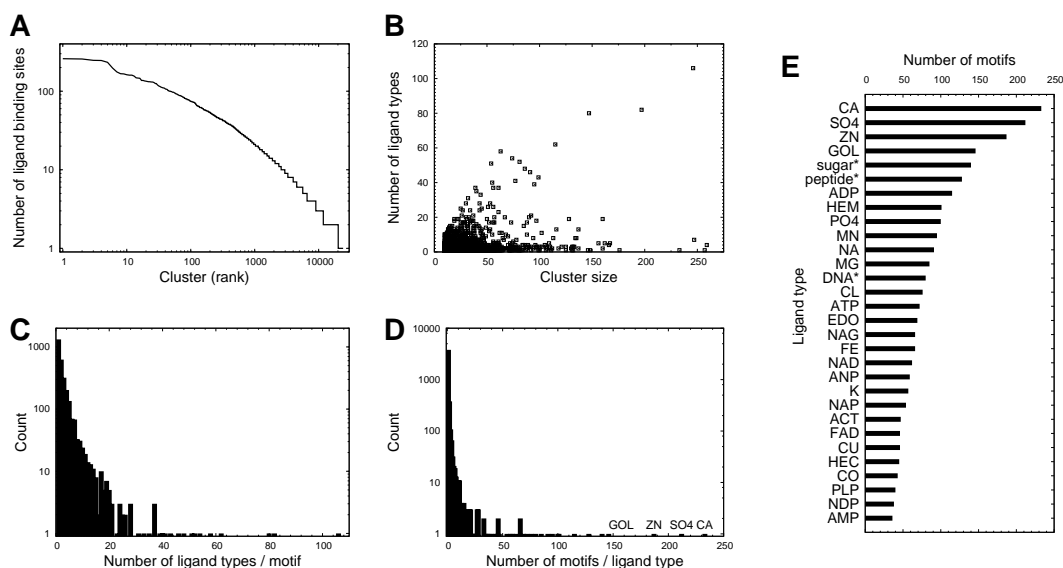


Fig. 3. Statistical properties of structural motifs. **A**: Size of complete-linkage clusters defined with P-value thresholds of 10^{-15} . **B**: Scatter plot of cluster size versus ligand types found in cluster. **C**: Histogram of the number of ligand types per structural motif (cluster). **D**: Histogram of the number of structural motifs (clusters) associated with a given ligand type. **E**: 30 most abundant ligand types (polymer molecules are marked with an asterisk).

128,484 (69%) of all the 186,485 sites. Out of these clusters, 2959 clusters consisted of at least 10 sites, accounting for 69,748 (37%) sites. The list of these clusters of structural motifs is available on-line². Since the ligand binding sites in small clusters are not reliable due to statistical errors, we use only the 2959 clusters consisting of at least 10 sites in the following analysis unless otherwise stated.

Diversity of structural motifs with respect to ligand types

Although some structural motifs included binding sites for a wide variety of ligand types, this is not always the case (Fig. 3B). Here, each PDB chemical component identifier (consisting of 1 to 3 letters) corresponds to a ligand type except for peptides, nucleic acids or sugars, which were treated simply as such (i.e., polymer sequence identity is ignored). Large clusters associated with many kinds of ligands were almost always enzymes such as proteases (eukaryotic or retroviral), carbonic anhydrases, protein kinases and protein phosphatases, whose structures have been solved with a variety of inhibitors. For example, two structural motifs consisting of 246 and 147 ligand binding sites of eukaryotic (trypsin-like) proteases were associated with 106 and 80 ligand types, respectively; two motifs consisting of 197 and 115 sites of retroviral proteases with 82 and 62 ligand types, respectively; a motif of 63 sites of protein kinases with 58 ligand types. On the contrary, large clusters with a limited variety of ligands were binding sites for heme (globins and nitric oxide synthase oxygenases) or

metal ions. Each structural motif is associated with 3.2 ligand types on average (standard deviation 5.3): 1322 motifs (47%) with only one ligand type and 2807 motifs (95%) with less than 10 ligand types whereas only 34 motifs contained more than 20 ligand types (Fig. 3C). In general, the diversity of ligand types per structural motif is low.

The converse is also true. That is, the number of structural motifs associated with each ligand type is generally very limited with the average of 2.1 motifs (standard deviation 8.4) per ligand type (Fig. 3D), and 3791 ligand types correspond to single motifs. Nevertheless, there were some ligands which were associated with many motifs (Fig. 3E). As expected, ligands often included in the solvent (e.g., SO4 [sulfate], MG [magnesium ion], GOL [glycerol], EDO [ethanediol]) were found in many motifs. Reflecting a large number of possible sequences, polymer molecules including peptide, sugar, and DNA were also found to be bound with many motifs, respectively. Other than these, mononucleotides and dinucleotides and metal ions exhibited a wide range of binding modes.

Diversity with respect to protein families and folds. Not many, but some structural motifs were found to contain ligand binding sites of distantly related proteins. To quantitatively analyze the diversity of structural motifs in terms of homologous families and global structural similarities, we assigned protein family, superfamily, fold and classes to each structural motif according to the SCOP (Murzin *et al.*, 1995) database. More concretely, the most specific SCOP code (SCOP concise classification string, SCCS) was assigned to each motif that was shared by all

² <http://pdbs6.pdbj.org/~akinjo/lbs/cluster.xml>

members of the corresponding cluster when it was possible, otherwise (i.e., there is at least one member that is different from other members in the cluster at the class level), motif was categorized as “others” (Fig. 4A).

Out of 2705 motifs to which SCCS can be assigned, 2637 and 62 motifs shared the same domains at the family and superfamily level, respectively. Thus, more than 99% of the motifs (of at least 10 binding sites) only contained binding sites of evolutionarily related proteins. One motif contained proteins from different superfamilies but of the same fold. This motif corresponded to the heme binding site of heme-binding four-helical bundle proteins (SCOP: f.21). Five motifs accommodated similarities across different folds, out of which three were zinc binding motifs (Krishna *et al.*, 2003). One motif contained a P-loop motif which is shared between the P-loop containing nucleotide triphosphate hydrolases (NTH) (SCOP: c.37) and the PEP carboxykinase-like fold (SCOP: c.91) (Fig. 5A) (Tari *et al.*, 1996). One motif was of the nucleotide-binding sites from FAD/NAD(P)-binding domain (SCOP: c.3) and Nucleotide-binding domain (SCOP: c.4) (Fig. 5B). Note that some PDB entries have not yet been annotated in SCOP. Currently, if such members exist in a cluster, they are simply ignored, and the assigned SCCS is based only on the members whose SCCS is known. Therefore, the number of motifs not sharing the same folds is somewhat underestimated. Nevertheless, it seems a general tendency that most motifs are confined within homologous proteins, namely families or superfamilies.

It was shown above that sequence similarity was only weakly related to the structural similarity of ligand binding sites (Fig. 2). This point can be further clarified by examining motifs of similar binding sites of related proteins. For example, the peptide binding sites of a pig trypsin (PDB: 1UHB (Pattabhi *et al.*, 2004)) and of a human hepsin (PDB: 1Z8G (Herter *et al.*, 2005)) were both in the same cluster but they share little sequence similarity (5% sequence identity based on a structural alignment (Kawabata & Nishikawa, 2000; Kawabata, 2003)), while the peptide binding site of bovine trypsin (PDB: 1QB1 (Whitlow *et al.*, 1999)) in another cluster shares 81% sequence identity with the pig thrombin in the previous cluster. This observation can be explained by the fact that different motifs cover different regions of proteins even though they are spatially close or even partially overlapping. The same argument applies to other motifs of related proteins. Thus, the structural motifs distinguish subtle differences in ligand binding site structures independent of sequence similarity.

It has been known that some protein folds can accommodate a wide range of functions. It is expected that the diversity of function is reflected in that of structures of ligand binding sites. To analyze such tendency, we counted the number of motifs that belong to each protein fold (Fig. 4B). Only a handful of folds showed a large diversity in terms of structural motifs. On average, 8.9 motifs were assigned to a fold. Out of 332 folds used in the analysis,

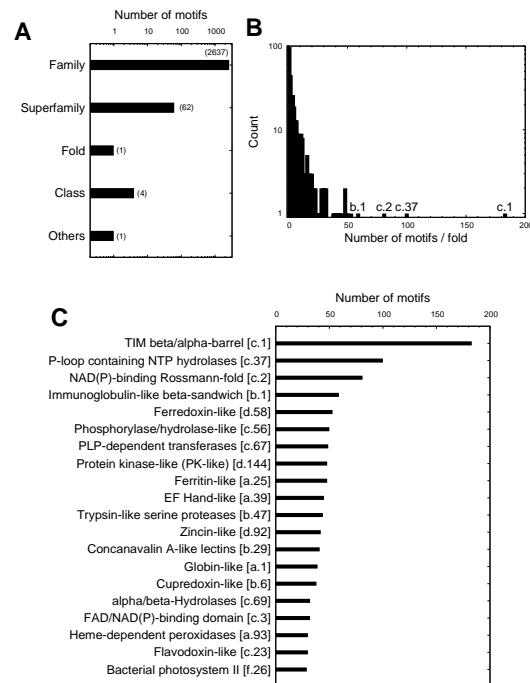


Fig. 4. Diversity of structural motifs in terms of protein folds. **A**: Number of motifs to which the given SCOP (Murzin *et al.*, 1995) hierarchical level (family, superfamily, fold, class) can be assigned. **B**: Histogram of the number of structural motifs associated with each SCOP fold. **C**: 20 most diverse SCOP folds in terms of the number of associated structural motifs.

only 18 contained more than 30 motifs (Fig. 4C). Among them, the TIM barrel fold was an extreme case with 183 motifs assigned, reflecting the great diversity of its functions (Nagano *et al.*, 2002). Some superfolds (Orengo *et al.*, 1994) such as Rossmann-fold, immunoglobulin-like, globin-like, etc. also showed great diversities of ligand binding sites.

Similarity network of ligand binding sites While each motif defines a precise pattern of ligand binding mode, the members of different structural motifs share significant structural similarities with each other. To explore the global structure of the ‘ligand binding site universe,’ we constructed a similarity network based on the results of the all-against-all comparison. Each structural motif was represented as a node and two nodes were connected if a member of one node was significantly similar to a member of the other node (i.e., the P-value of their alignment was below a predefined threshold). Thus constructed network can be decomposed into a number of connected components. When the threshold was greater than 10^{-14} , the size of the largest connected component of the network was one or two orders of magnitude greater than that of the second largest one (Fig. 6A). For example, setting the threshold to 10^{-10} yielded the largest connected component consisting of 78,190 sites (i.e., 42% of 186,485 sites). Accordingly,

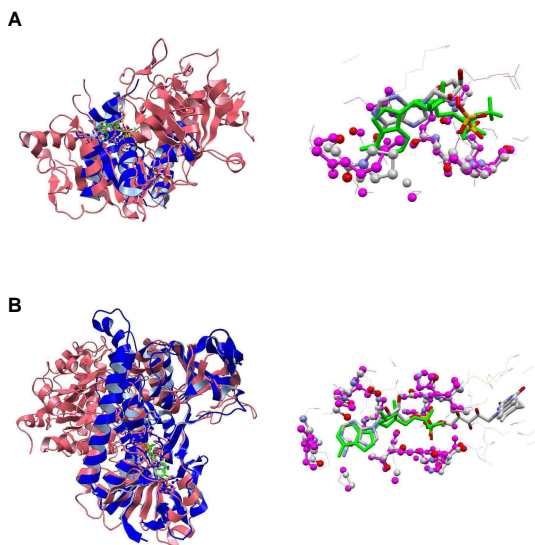


Fig. 5. Examples of structural motifs shared by different protein folds. The left panel shows the whole protein structures (colored in blue or pink) superimposed based on the alignment of the ligand binding sites shown in the right panel (colored in the CPK scheme or magenta (protein) and green (ligand), respectively). **A:** ADP binding site of bacterial shikimate kinase (PDB: 2DFT (Dias *et al.*, 2007); SCOP: c.37; blue / CPK-colored) and ATP binding site of bacterial phosphoenolpyruvate carboxykinase (PDB: 1AQ2 (Tari *et al.*, 1997); SCOP: c.91; pink / protein in magenta, ADP in green). **B:** FAD binding site of human glutathione reductase (PDB: 5GRT (Stoll *et al.*, 1997); SCOP: c.3; blue / CPK-colored) and ADP binding site of bacterial trimethylamine dehydrogenase (PDB: 2TMD (Barber *et al.*, 1992); SCOP: c.4; pink / protein in magenta, ADP in green).

many functionally unrelated binding sites were somehow connected in the largest component, which complicated the interpretation of the component. With the P-value threshold of 10^{-15} or less, the first several connected components were of the same order (Fig. 6A), and many members of each component appeared to be more functionally related. Thus, we set $P = 10^{-15}$ for constructing the network in the following (as well as for defining the complete-linkage clusters described above).

Excluding 54,092 singleton components (those consisting of only one site), 11,532 connected components were found. The largest component consisted of 7935 sites, and 1881 components contained at least 10 sites (Fig. 6A).

The main constituents of the largest connected component of the similarity network (Fig. 6B) were mononucleotide (ADP, GDP, etc.) or phosphate binding (PO₄) sites. Most notable were P-loop containing NTH (SCOP: c.37) and PEP carboxykinases (SCOP: c.91) which formed a closely connected group as they share similar phosphate binding sites, i.e., the P-loop motif (the term ‘group’ used here indicates closely connected clusters in a network component colored in green in Fig. 6B-F). Directly connected with this group was the coenzyme A (CoA) binding site of acetyl-CoA acetyltransferases. The magnesium ion (MG) binding site of Ras-related proteins were also connected with the group of the P-loop containing proteins since the magnesium ion is often located near the phosphate binding

site. Mononucleotide or phosphate (AMP, U5P, PRP, PO₄) binding sites of various phosphoribosyltransferases and the flavin mononucleotide (FMN) binding site of flavodoxins were also closely connected. The phosphate binding site of tyrosine-protein phosphatases formed another group which was weakly connected to the FMN binding site of flavodoxins.

It is surprising that the heme binding site of globins (hemoglobins, myoglobins, cytoglobins, etc.) was also included in this component. Nevertheless, it was not directly connected to the main group of P-loops, but indirectly via the sparse group consisting of chloride ion binding site of T4 lysozymes and sulphate and phosphate binding sites of miscellaneous proteins. The binding sites of this latter group were made of regular structures at the termini of α -helices. When we used a more stringent P-value threshold (say, 10^{-20}), the groups of globins and lysozymes were detached from the main group, but the main group containing the P-loops was almost unaffected (data not shown). Thus, the matches connecting globins, lysozymes, and P-loop containing proteins may be considered as ‘false’ hits. Based solely on structural similarity, however, they are difficult to discriminate from ‘true’ hits (structural matches between functionally related sites) since many functional sites often include regular structures at termini of secondary structures. Nevertheless, the fact that only a subset of regular structures were detected suggests that these matches may correspond to recurring structural patterns often used as building blocks of functional sites. In addition, we point out that weak but meaningful enzymatic functions are sometimes detected experimentally in such ‘false’ hits (Ikura *et al.*, 2008).

The second largest connected component mainly consisted of mononucleotides or dinucleotides binding sites of the so-called Rossmann-like fold domains (Fig. 6C) which include, among others, NAD(P)-binding Rossmann-fold domains (SCOP: c.2), FAD/NAD(P)-binding domain (SCOP: c.3), nucleotide-binding domain (SCOP: c.4), SAM-dependent methyltransferases (SCOP: c.66), activating enzymes of the ubiquitin-like proteins (SCOP: c.111) and urocanase (SCOP: e.51).

Peptide (and inhibitor) binding sites of trypsin-like and subtilisin-like proteases were found in the third largest component (Fig. 6D). These two proteases do not share a common fold, but were connected due to the similarity of the active site structures around the well-known catalytic triad.

The EF hand motif, a major calcium binding motif, was found in the fourth largest component (Fig. 6E) in which a variety of other calcium ion binding sites were also found. Although the main group in this component mainly consisted of the calcium ion binding sites of various calmodulin-like proteins, it also contained similar sites of periplasmic binding proteins (PBP). The ligands of these PBP’s also include sodium in addition to calcium ions. The main group was weakly connected to calcium ion binding sites of proteins of completely different folds such as galactose-binding domains (e.g., galactose oxidase, fucolectins), laminin G-

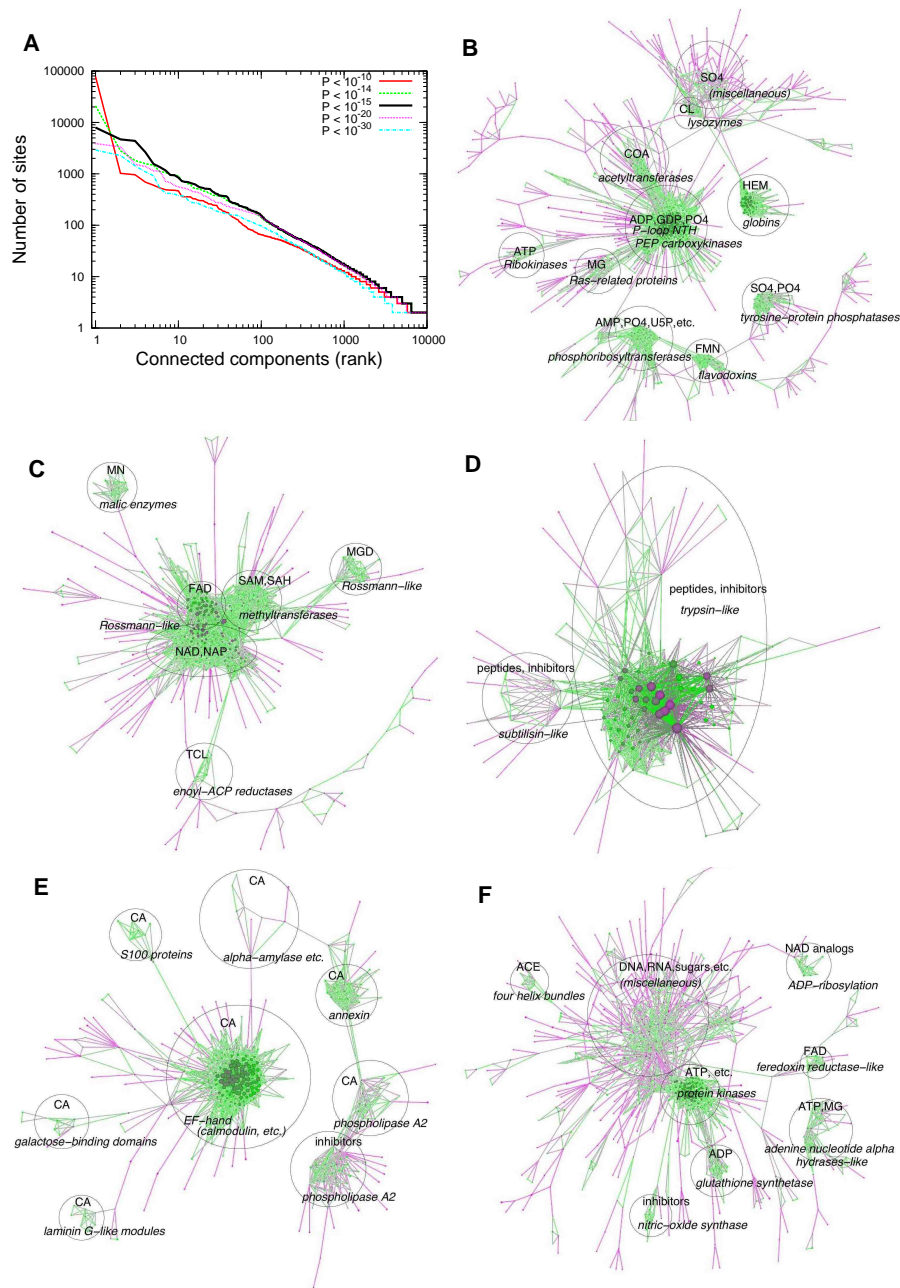


Fig. 6. Networks of structural motifs of ligand binding sites. **A**: Distribution of the size of connected component of the similarity network with varying P-value thresholds. A transition is observed at $P=10^{-15}$. **B-F**: The five largest connected components of the similarity network (P -value threshold = 10^{-15}). Some groups of structural motifs are marked by black circles annotated with ligand types and protein folds. To facilitate visualization, each node (shown as a sphere) is represented as a complete-linkage cluster (structural motif) of ligand binding sites defined with $P = 10^{-15}$ (the sphere size is proportional to the cluster size). Nodes and edges are colored according to the values of their clustering coefficient (green: high; magenta: low) (Watts & Strogatz, 1998).

like modules (e.g., laminin, agrin, etc.), alpha-amylases, annexins, and phospholipase A2. Due to its spatial proximity, the calcium binding site of phospholipase A2 was also connected to its inhibitor binding sites.

Our last example, the fifth largest component, exhibited an exploding structure (Fig. 6F). Nevertheless, most binding sites are associated with nucleotides. The main closely connected group consisted of the ATP (and inhibitors) binding sites of protein kinase family proteins, next to

which the ADP binding sites of glutathione synthetase family proteins (including D-ala-D-ala ligases) were connected. Other closely connected groups included FAD binding sites of ferredoxin reductase-like proteins, ATP or magnesium binding sites of adenine nucleotide alpha hydrolases-like proteins, inhibitor binding sites of nitric-oxide synthases, and NAD (analog) binding sites of ADP-ribosylation proteins (e.g., T-cell ecto-ADP-ribosyltransferase 2, iota toxin, etc.). There was a large sparse group connected with the

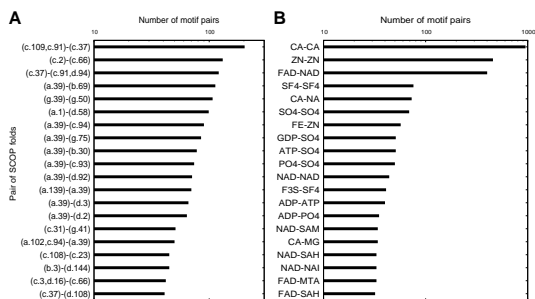


Fig. 7. Ligand binding sites shared across different protein folds. **A**: 20 most common pairs of different folds sharing significant ligand binding site similarities. **B**: 20 most common pairs of ligand types shared across different folds.

main group of protein kinases. In that sparse group, ligand binding sites of transthyretins (prealbumins) were often found to be directly connected with that of protein kinases although their folds are different. These binding sites both involve a face of a β -sheet, and their similarity was found due to the backbone conformation of the β -sheet. Since many proteins bind their ligands on a face of a β -sheet, this observation in turn explains the origin of the large sparse group.

Significant similarities across different folds The similarity network of ligand binding sites revealed many structural similarities across different folds. To explore the extent of significant ‘cross-fold’ similarities (with $P < 10^{-15}$), we assigned SCOP codes to as many structural motifs as possible, and enumerated motif pairs whose members were significantly similar but did not share a common fold (Fig. 7A). We also examined the ligand pairs in those matches, and found that most of them were reasonable matches (Fig. 7B): metal ions were matched with metal ions, nucleotides with nucleotides or phosphate, and so on. Thus, many of these cross-fold similarities are expected to be functionally relevant. The observation that sulfate (SO4) binding sites were often found to be matched with mononucleotide (GDP and ATP) or phosphate (PO4) binding sites (Fig. 7B) confirms the usefulness of the former ligand in inferring the binding of the latter ligands, as often practiced by crystallographers. We note that multiple SCCS may be assigned to a single motif if it contains multiple fold types or its member sites are located at an interface of multiple domains. In order to cover all possible fold pairs, we did not exclude motifs consisting of less than 10 binding sites in this analysis. There were in total 4035 pairs of structural motifs (52,709 pairs of binding sites) that exhibited significant similarities but did not share the same fold. The complete list of these pairs is available on-line³.

The most common cross-fold similarity was found between the P-loop containing NTH (SCOP: c.37) and the

PEP-carboxykinase-like (SCOP: c.91) (c.f. Fig. 5A). As described in the analysis of complete-linkage clusters, this corresponds to mononucleotide or phosphate binding sites.

Mononucleotide or dinucleotide binding sites of various Rossmann-like folds (SCOP: c.2, c.3, c.4, c.66) also exhibited significant mutual similarities (e.g., Figs. 5B and 8A).

The calcium binding sites of EF hand-like fold (a.39) were found to be similar to the metal binding sites of many folds including beta-propeller proteins (Fig. 8B) and periplasmic binding proteins (SCOP: c.93 [class I], c.94 [class II]), lysozyme-like (SCOP: d.2), Zincin-like (SCOP: d.92), and many others.

Similar zinc binding sites were found in many, mostly small, folds in addition to DHS-like NAD/FAD-binding domain (SCOP: c.31) and Rubredoxin-like (g.41) (Fig. 8C), the former of which may be regarded as an inserted zinc finger motif.

The similarity between globin-like (SCOP: a.1) and ferredoxin-like (SCOP: d.58) was due to the coordinated structures of the iron-sulfur clusters found in alpha-helical ferredoxins and ferredoxins, respectively.

HAD-like fold proteins (SCOP: c.108) and CheY-like (flavodoxin fold) proteins (SCOP: c.23) often share similar binding sites (e.g., Fig. 8D). Interestingly, although these proteins have very similar topologies, the orders of aligned secondary structure elements were different when the alignment was based on the ligand binding site similarity.

As noted in the description of a network component (Fig. 6F), protein kinases and transthyretins share similar binding sites which are located on a face of a β -sheet (Fig. 8E). Nevertheless, their ligand moieties seem also similar.

Also as seen in the network component (Fig. 6B), phosphate binding site of the P-loop motif exhibits a significant similarity with CoA binding site of acetyltransferases (Fig. 8F). A close examination showed the phosphate bound to the P-loop motif coincided with the phosphate group of CoA bound to the acetyltransferase.

The list of the cross-fold similarities contained many other examples including, but not limited to, those discussed in the context of the similarity network. Here we give two other examples. Bacterial peptide deformylase 2 (SCOP: d.167) and human macrophage metalloelastase (SCOP: d.92) both act with peptides, and their ligand binding sites exhibit high structural similarity (Fig. 8G). DNA is one of the most abundant ligands found in cross-fold similarities (Fig. 7B). Not surprisingly, there can be also found similarity between binding sites for DNA and RNA. One example is the KH1 domain of human poly(rC)-binding protein 2 which binds DNA and bacterial transcription elongation protein NusA which binds RNA (Fig. 8H). These proteins have different variants of the KH domains (Grishin, 2001b).

³ <http://pdjbs6.pdbj.org/~akinjo/lbs/diffold.xml>

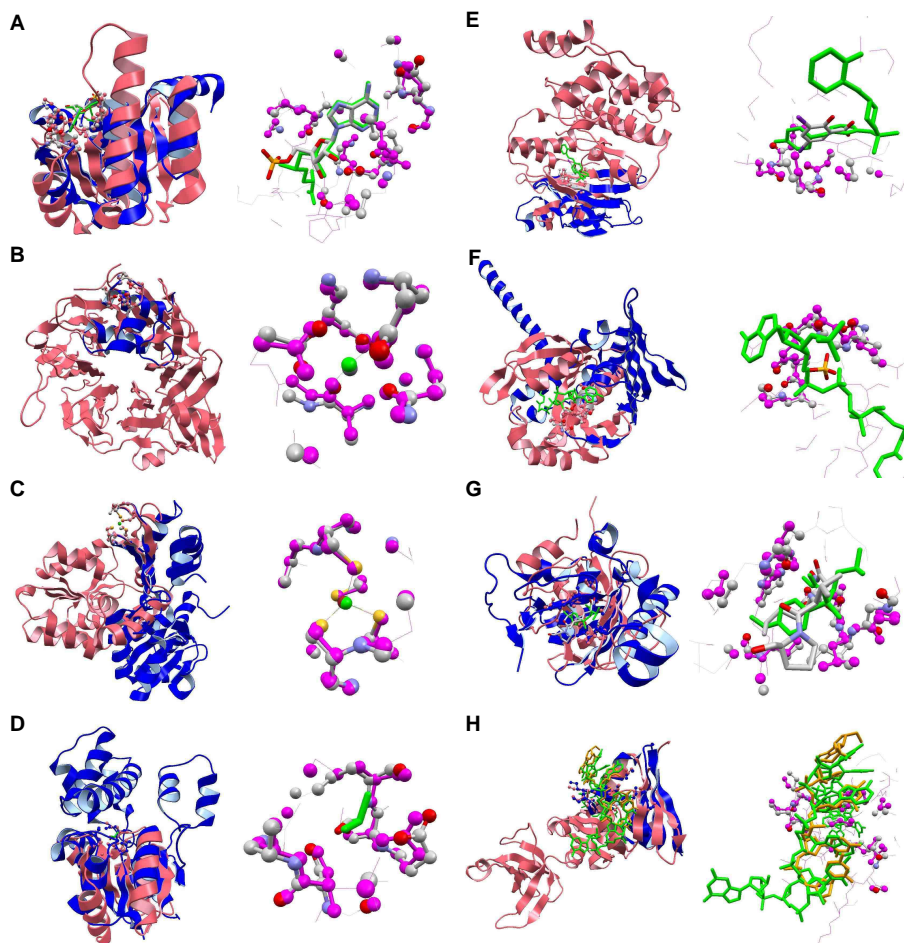


Fig. 8. Examples of ligand binding sites shared across different folds. The color schemes are the same as in Fig. 5. **A:** AMP binding site of *Thermotoga maritima* hypothetical protein tm1088a (PDB: 2G1U (Joint Center for Structural Genomics, 2006); SCOP: c.2; blue / CPK-colored) and SAM binding site of human putative ribosomal RNA methyltransferase 2 (PDB: 2NYU (Wu *et al.*, 2006); SCOP: c.66; pink / protein in magenta, SAM in green). **B:** Calcium binding sites of *Clostridium thermocellum* cellulosomal scaffolding protein A (PDB: 2CCL (Carvalho *et al.*, 2007); SCOP: a.39; blue / CPK-colored) and human integrin alpha-IIb (PDB: 1TXV (Xiao *et al.*, 2004); SCOP: b.69; pink / protein in magenta, calcium in green). **C:** Zinc binding sites of human NAD-dependent deacetylase (PDB: 2H4H (Hoff *et al.*, 2006); SCOP: c.31 [inferred by SSM (Krissinel & Henrick, 2004)]; blue / CPK-colored) and *Bacillus stearothermophilus* adenylate kinase (PDB: 1ZIN (Berry & Phillips Jr., 1998); SCOP: g.41; pink / protein in magenta, zinc in green). **D:** Formic acid binding site of *Xanthobacter autotrophicus* L-2-haloacid dehalogenase (PDB: 1AQ6 (Ridder *et al.*, 1997); SCOP: c.108; blue / CPK-colored) and BeF_3^- binding site of *Escherichia coli* PhoB (PDB: 1ZES (Bachhawat *et al.*, 2005); SCOP: c.23; pink / protein in magenta, BeF_3^- in green). **E:** 3,5-diiodosalicylic acid binding site of human transthyretin (PDB: 3B56; SCOP: b.3; blue / CPK-colored) and inhibitor (N-[3-(4-fluorophenoxy)phenyl]-4-[(2-hydroxybenzyl)amino]piperidine-1-sulfonamide) binding site of human mitogen-activated protein kinase 14 (PDB: 1ZZ2; SCOP: d.144; pink / protein in magenta, inhibitor in green). **F:** phosphate binding site of *Pyrococcus furiosus* Rad50 ABC-AT-Pase (PDB: 1II8; SCOP: c.37; blue / CPK-colored) and coenzyme-A (CoA) binding site of *Salmonella typhimurium* LT2 acetyl transferase (PDB: 1S7N; SCOP: d.108; pink / protein in magenta, CoA in green). **G:** Actinonin binding site of *B. stearothermophilus* peptide deformylase 2 (PDB: 1LQY (Guilloteau *et al.*, 2002); SCOP: d.167; blue / CPK-colored) and NNGH binding site of human macrophage metalloelastase (PDB: 1Z3J; SCOP: d.92; pink / protein in magenta, NNGH in green). **H:** DNA binding site of KH1 domain of human poly(rC)-binding protein (PDB: 2AXY (Du *et al.*, 2005); SCOP: d.51; blue / CPK-colored, DNA in orange) and RNA binding site of *Mycobacterium tuberculosis* transcription elongation protein NusA (PDB: 2ATW (Beuth *et al.*, 2005); SCOP: d.52; pink / protein in magenta, RNA in green).

all comparison, we were able to obtain an extensive list of ligand binding site similarities irrespective of sequence homology or global protein fold. The similarity network uncovered very many cross-fold similarities as well as well-known ones. Although it is still not clear how many of these similarities are functionally relevant, it was often observed that different folds were superimposable to a significant extent when the alignment was based on the ligand binding sites (e.g., Figs. 5, 8). Aligning protein

structures based on ligand binding sites (or functional sites in general) irrespective of sequence similarity, sequence order, and protein fold (as currently defined) may be a useful approach to elucidating the evolutionary history of fold changes (Grishin, 2001a; Krishna & Grishin, 2004; Andreeva & Murzin, 2006; Taylor, 2007; Goldstein, 2008; Xie & Bourne, 2008).

As was seen in the similarity network (Fig. 6), some links are based on the similarity of highly regular (secondary)

structures which are found in many protein structures (e.g., Fig. 6B,F). While such similarities may not be directly related to any biochemical functions, they suggest that many ligand binding sites are based on combinations of some regular local structures. It is known that a relatively small library of backbone fragments can accurately model tertiary structures of proteins (Kolodny *et al.*, 2002). Consequently, the variety of contiguous fragments recurring in ligand binding sites is also limited as far as backbone structure is concerned. Friedberg & Godzik (2005) found similarities across different protein folds including those involved in various zinc-finger motifs and Rossmann-like folds, as shown in this study. They also showed significant correlations between similarity of fragments and that of protein functions. This observation is consistent with the present results in that it suggests that specific combinations of fragments encode specific functions. To apply the GIRAF method to functional annotations, however, it is preferable to discriminate functionally relevant similarities from purely structural similarities.

Some of the short-comings of simple pairwise comparison may be overcome by the complete-linkage clustering analysis of similar binding sites, which allowed us to define precise structural motifs. It should be stressed that defining reliable motifs requires redundancy in the PDB (Wangikar *et al.*, 2003), otherwise it would be more difficult to distinguish recurring structures from incidental matches. These motifs may be useful for defining structural templates for efficient motif matching (Wallace *et al.*, 1997). Despite the diversity of binding sites and their similarities, most motifs were found to be confined within single families or superfamilies, and they were also found to be highly specific to particular ligands. Thus, these motifs may be helpful for annotating putative functions of proteins, especially, of structural genomics targets.

In conclusion, the development of an extremely efficient search method (GIRAF) to detect local structural similarities made it possible to conduct the first exhaustive all-against-all comparison of all ligand binding sites in all the known protein structures. We identified a number of well-defined structural motifs, enumerated many non-trivial similarities. While exhaustive pairwise comparisons are useful for detecting weak and possibly partial similarities between ligand binding sites, the significance of such matches may not be immediately obvious because some of them may be based on ubiquitous regular structures.

Meanwhile, complete-linkage clusters of ligand binding sites are useful for identifying functionally relevant binding site structures, but they may neglect partial but significant matches. Therefore, these two approaches, exhaustive pairwise comparison and motif matching, are complementary to each other, and hence the combination thereof may be helpful for more reliable annotations of proteins with unknown functions. These approaches may be further supplemented by other existing fold and/or sequence-based methods (Standley *et al.*, 2008; Xie & Bourne, 2008). The present method can be also applied to a whole protein

structure (not limited to its predefined ligand binding sites) to find potential ligand binding sites (Kinjo & Nakamura, 2007). In this way, we are currently annotating all structural genomics targets (Chen *et al.*, 2004). We also plan to make this method available as a web service so that structural biologists can routinely search for ligand binding sites of their interest.

Experimental Procedures

The GIRAF method The details of the original GIRAF method has been published elsewhere (Kinjo & Nakamura, 2007). In this study, an improved version of GIRAF was used for conducting the all-against-all comparison. The improvement includes more sensitive geometric indexing with atomic composition around each reference set, simplified SQL expressions, and parallelization (A.R.K. and H.N., unpublished).

All-against-all comparison Ligand binding sites were extracted from PDBML files as described in Results. A ligand is defined as those entities that are annotated neither as “polypeptide(L)” with more than 24 amino acid residues nor “water” in the entity category. That is, a ligand can be polypeptide shorter than 25 residues, DNA, RNA, polysaccharides (sugars), lipids, metal ions, iron-sulfur clusters, or any other small molecules. However, ligands with more than 1000 atoms were discarded. The all-against-all comparison was carried out on a cluster machine consisting of 20 nodes of 8-core processors (Intel Xeon 3.2 GHz). The whole computation was finished within approximately 60 hours.

Clusters of similar ligand binding sites

To obtain complete-linkage clusters, we first constructed a single-linkage network based on a pre-defined P-value threshold. Then this network was decomposed into connected components. Each component was then broken into finer components by imposing a more stringent P-value threshold. This decomposition was iterated until P-value threshold reached 10^{-100} . Then bottom-up complete-linkage was iteratively applied to each connected component, the result of which was then combined into an upper component (previously determined with a higher P-value threshold). This bottom-up process was terminated when P-value threshold, 10^{-15} , was reached. Each cluster was defined as a structural motif for the ligand binding sites.

Analysis of networks and structural motifs

To annotate thus obtained structural motifs with the SCOP (Murzin *et al.*, 1995) codes, we used the parsable file of SCOP (version 1.73). When an analysis involved SCOP codes, those PDB entries whose SCOP classification has not yet been determined were ignored. Each SCOP SCCS code was assigned to a ligand binding site as described by others (Gold & Jackson, 2006). When a site resides at an interface of multiple domains, multiple SCCS codes were assigned to the site. Two or more binding sites are said to share the same fold (or family, superfamily, etc.) if the intersection of their SCCS code sets is not empty. The SCCS code assigned to a structural motif was defined as the union of all the SCCS codes found in the corresponding cluster members. We used only the seven main SCOP classes (all- α [a], all- β [b], α/β [c], $\alpha + \beta$ [d], multi-domain [e], membrane and cell surface proteins and peptides [f], and small proteins [g]). The figures of alignments (Figs. 5 and 8) were created with jV version 3 (Kinoshita & Nakamura, 2004) using the PDBML-extatom files produced by GIRAF. The network figures (Fig. 6B-F) were created with the Tulip software (<http://www.tulip-software.org/>).

References

- Altschul, S. F., Madden, T. L., Schaffer, A. A., Zhang, J., Zhang, Z., Miller, W., & Lipman, D. L. (1997). Gapped blast and PSI-blast: A new generation of protein database search programs. *Nucleic Acids Res.* *25*, 3389–3402.
- Andreeva, A. & Murzin, A. G. (2006). Evolution of protein fold in the presence of functional constraints. *Curr. Opin. Struct. Biol.* *16*, 399–408.
- Bachhawat, P., Swapna, G. V., Montelione, G. T., & Stock, A. M. (2005). Mechanism of activation for transcription factor PhoB suggested by different modes of dimerization in the inactive and active states. *Structure* *13*, 1353–1363.
- Barber, M. J., Neame, P. J., Lim, L. W., White, S., & Matthews, F. S. (1992). Correlation of X-ray deduced and experimental amino acid sequences of trimethylamine dehydrogenase. *J. Biol. Chem.* *267*, 6611–6619.
- Berman, H., Henrick, K., Nakamura, H., & Markley, J. L. (2007). The worldwide Protein Data Bank (wwPDB): ensuring a single, uniform archive of PDB data. *Nucleic Acids Res.* *35*, D301–D303.
- Berry, M. B. & Phillips Jr., G. N. (1998). Crystal structures of *Bacillus stearothermophilus* adenylate kinase with bound Ap5A, Mg²⁺ Ap5A, and Mn²⁺ Ap5A reveal an intermediate lid position and six coordinate octahedral geometry for bound Mg²⁺ and Mn²⁺. *Proteins* *32*, 276–288.
- Beuth, B., Pennell, S., Arnvig, K. B., Martin, S. R., & Taylor, I. A. (2005). Structure of a *Mycobacterium tuberculosis* NusA-RNA complex. *EMBO J.* *24*, 3576–3587.
- Brakoulias, A. & Jackson, R. M. (2004). Towards a structural classification of phosphate binding sites in protein-nucleotide complexes: an automated all-against-all structural comparison using geometric matching. *Proteins* *56*, 250–260.
- Carvalho, A. L., Dias, F. M. V., Nagy, T., Prates, J. A. M., Proctor, M. R., Smith, N., Bayer, E. A., Davies, G. J., Ferreira, L. M. A., Romao, M. J., Fontes, C. M. G. A., & Gilbert, H. J. (2007). Evidence for a dual binding mode of dockerin modules to cohesins. *Proc. Natl. Acad. Sci. USA* *104*, 3089–3094.
- Chen, L., Oughtred, R., Berman, H. M., & Westbrook, J. (2004). TargetDB: a target registration database for structural genomics projects. *Bioinformatics* *20*, 2860–2862.
- Dias, M. V., Faim, L. M., Vasconcelos, I. B., de Oliveira, J. S., Basso, L. A., Santos, D. S., & de Azevedo, W. F. (2007). Effects of the magnesium and chloride ions and shikimate on the structure of shikimate kinase from *Mycobacterium tuberculosis*. *Acta Crystallogr. F* *63*, 1–6.
- Du, Z., Lee, J. K., Tjhen, R., Li, S., Pan, H., Stroud, R. M., & James, T. L. (2005). Crystal structure of the first kh domain of human poly(C)-binding protein-2 in complex with a C-rich strand of human telomeric DNA at 1.7 Å. *J. Biol. Chem.* *280*, 38823–38830.
- Friedberg, I. & Godzik, A. (2005). Connecting the protein structure universe by using sparse recurring fragments. *Structure* *13*, 1213–1224.
- Garcia-Molina, H., Ullman, J. D., & Widom, J. (2002). *Database Systems: The Complete Book* (Prentice Hall: Upper Saddle River, NJ, U. S. A.).
- Gold, N. D. & Jackson, R. M. (2006). Fold independent structural comparisons of protein-ligand binding sites for exploring functional relationships. *J. Mol. Biol.* *355*, 1112–1124.
- Goldstein, R. A. (2008). The structure of protein evolution and the evolution of protein structure. *Curr. Opin. Struct. Biol.* *18*, 170–177.
- Gonzalez, B., Schell, M. J., Letcher, A. J., Veprintsev, D. B., Irvine, R. F., & Williams, R. L. (2004). Structure of a human inositol 1,4,5-trisphosphate 3-kinase: substrate binding reveals why it is not a phosphoinositide 3-kinase. *Mol. Cell* *15*, 689–701.
- Grishin, N. V. (2001a). Fold change in evolution of protein structures. *J. Struct. Biol.* *134*, 167–185.
- Grishin, N. V. (2001b). KH domain: one motif, two folds. *Nucleic Acids Res.* *29*, 638–643.
- Guilloteau, J. P., Mathieu, M., Giglione, C., Blanc, V., Dupuy, A., Chevrier, M., Gil, P., Famechon, A., Meinel, T., & Mikol, V. (2002). The crystal structures of four peptide deformylases bound to the antibiotic actinonin reveal two distinct types: a platform for the structure-based design of antibacterial agents. *J. Mol. Biol.* *320*, 951–962.
- Gutteridge, A. & Thornton, J. M. (2005). Understanding

- nature's catalytic toolkit. *Trends Biochem. Sci.* *30*, 622–629.
- Herter, S., Piper, D. E., Aaron, W., Gabriele, T., Cutler, G., Cao, P., Bhatt, A. S., Choe, Y., Craik, C. S., Walker, N., Meininger, D., Hoey, T., & Austin, R. J. (2005). Hepatocyte growth factor is a preferred in vitro substrate for human hepsin, a membrane-anchored serine protease implicated in prostate and ovarian cancers. *Biochem. J.* *390*, 125–136.
- Hoff, K. G., Avalos, J. L., Sens, K., & Wolberger, C. (2006). Insights into the sirtuin mechanism from ternary complexes containing NAD⁺ and acetylated peptide. *Structure* *14*, 1231–1240.
- Ikura, T., Kinoshita, K., & Ito, N. (2008). A cavity with an appropriate size is the basis of the ppiase activity. *Protein Eng. Des. Sel.* *21*, 83–89.
- Joint Center for Structural Genomics (2006). Crystal structure of (tm1088a) from *Thermotoga maritima* at 1.50 Å resolution. PDB entry 2G1U.
- Jones, S. & Thornton, J. M. (2004). Searching for functional sites in protein structures. *Curr. Opin. Struct. Biol.* *8*, 3–7.
- Kawabata, T. (2003). Matras: a program for protein 3D structure comparison. *Nucleic Acids Res.* *31*, 3367–3369.
- Kawabata, T. & Nishikawa, K. (2000). Protein tertiary structure comparison using the markov transition model of evolution. *Proteins* *41*, 108–122.
- Kinjo, A. R. & Nakamura, H. (2007). Similarity search for local protein structures at atomic resolution by exploiting a database management system. *BIOPHYSICS* *3*, 75–84. doi:10.2142/biophysics.3.75.
- Kinoshita, K. & Nakamura, H. (2004). eF-site and PDB-jViewer: database and viewer for protein functional sites. *Bioinformatics* *20*, 1329–1330.
- Kinoshita, K., Sadanami, K., Kidera, A., & Go, N. (1999). Structural motif of phosphate-binding site common to various protein superfamilies: all-against-all structural comparison of protein-monomonucleotide complexes. *Protein Eng.* *12*, 11–14.
- Kobayashi, N. & Go, N. (1997). ATP binding proteins with different folds share a common ATP-binding structural motif. *Nat. Struct. Biol.* *4*, 6–7.
- Kolodny, R., Koehl, P., Guibas, L., & Levitt, M. (2002). Small libraries of protein fragments model native protein structures accurately. *J. Mol. Biol.* *323*, 297–307.
- Krishna, S. S. & Grishin, N. V. (2004). Structurally analogous proteins do exist!. *Structure* *12*, 1125–1127.
- Krishna, S. S., Majumdar, I., & Grishin, N. V. (2003). Structural classification of zinc fingers: survey and summary. *Nucleic Acids Res.* *31*, 532–550.
- Krissinel, E. & Henrick, K. (2004). Secondary-structure matching (SSM), a new tool for fast protein structure alignment in three dimensions. *Acta Crystallogr. D* *60*, 2256–2268.
- Laronde-Leblanc, N., Guszczynski, T., Copeland, T., & Wlodawer, A. (2005). Autophosphorylation of *Archaeoglobus fulgidus* Rio2 and crystal structures of its nucleotide-metal ion complexes. *FEBS J.* *272*, 2800–2810.
- Lee, D., Redfern, O., & Orengo, C. (2007). Predicting protein function from sequence and structure. *Nat. Rev. Mol. Cell Biol.* *8*, 995–1005.
- Minai, R., Matsuo, Y., Onuki, H., & Hirota, H. (2008). Method for comparing the structures of protein ligand-binding sites and application for predicting protein-drug interactions. *Proteins* *72*, 367–381.
- Murzin, A. G., Brenner, S. E., Hubbard, T., & Chothia, C. (1995). SCOP: A structural classification of proteins database for the investigation of sequences and structures. *J. Mol. Biol.* *247*, 536–540.
- Nagano, N., Orengo, C. A., & Thornton, J. M. (2002). One fold with many functions: the evolutionary relationships between TIM barrel families based on their sequences, structures and functions. *J. Mol. Biol.* *321*, 741–765.
- Orengo, C. A., Jones, D. T., & Thornton, J. M. (1994). Protein superfamilies and domain superfolds. *Nature* *372*, 631–634.
- Pattabhi, V., Syed Ibrahim, B., & Shamaladevi, N. (2004). Trypsin activity reduced by an autocatalytically produced nonapeptide. *J. Biomol. Struct. Dyn.* *21*, 737–744.
- Polacco, B. J. & Babbitt, P. C. (2006). Automated discovery of 3D motifs for protein function annotation. *Bioinformatics* *22*, 723–730.
- Porter, C. T., Bartlett, G. J., & Thornton, J. M. (2004). The Catalytic Site Atlas: a resource of catalytic sites and residues identified in enzymes using structural data. *Nucleic Acids Res.* *32*, D129–D133.
- Ridder, I. S., Rozeboom, H. J., Kalk, K. H., Janssen, D. B., & Dijkstra, B. W. (1997). Three-dimensional structure of L-2-haloacid dehalogenase from *Xanthobacter autotrophicus* GJ10 complexed with the substrate-analogue formate. *J. Biol. Chem.* *272*, 33015–33022.
- Rognan, D. (2007). Chemogenomic approaches to rational drug design. *Br. J. Pharmacol.* *152*, 38–52.
- Shulman-Peleg, A., Nussinov, R., & Wolfson, H. J. (2004). Recognition of functional sites in protein structures. *J. Mol. Biol.* *339*, 607–633.
- Standley, D. M., Toh, H., & Nakamura, H. (2008). Functional annotation by sequence-weighted structure alignments: Statistical analysis and case studies from the Protein 3000 structural genomics project in Japan. *Proteins* *72*, 1333–1351.
- Stark, A. Sunyaev, S. & Russell, R. B. (2003). A model for statistical significance of local similarities in structure. *J. Mol. Biol.* *326*, 1307–1316.
- Stoll, V. S., Simpson, S. J., Krauth-Siegel, R. L., Walsh, C. T., & Pai, E. F. (1997). Glutathione reductase turned into trypanothione reductase: structural analysis of an engineered change in substrate specificity. *Biochemistry* *36*, 6437–6447.
- Tari, L. W., Matte, A., Goldie, H., & Delbaere, L. T. (1997). Mg²⁺-Mn²⁺ clusters in enzyme-catalyzed phosphoryl-transfer reactions. *Nat. Struct. Biol.* *4*, 990–994.
- Tari, L. W., Matte, A., Pugazhenthii, U., Goldie, H., &

- Delbaere, L. T. (1996). Snapshot of an enzyme reaction intermediate in the structure of the ATP-Mg²⁺-oxalate ternary complex of *Escherichia coli* PEP carboxykinase. *Nat. Struct. Biol.* *3*, 355–363.
- Taylor, W. R. (2007). Evolutionary transitions in protein fold space. *Curr. Opin. Struct. Biol.* *17*, 354–361.
- Wallace, A. C., Borkakoti, N., & Thornton, J. M. (1997). TESS: A geometric hashing algorithm for deriving 3D coordinate templates for searching structural databases. application to enzyme active sites. *Protein Sci.* *6*, 2308–2323.
- Wangikar, P. P., Tendulkar, A., Ramya, S., Mali, D. N., & Sarawagi, S. (2003). Functional sites in protein families uncovered via an objective and automated graph theoretic approach. *J. Mol. Biol.* *326*, 955–978.
- Watts, D. J. & Strogatz, S. (1998). Collective dynamics of ‘small-world’ networks. *Nature* *393*, 440–442.
- Westbrook, J., Ito, N., Nakamura, H., Henrick, K., & Berman, H. M. (2005). PDBML: the representation of archival macromolecular structure data in XML. *Bioinformatics* *21*, 988–992.
- Whitlow, M., Arnaiz, D. O., Buckman, B. O., Davey, D. D., Griedel, B., Guilford, W. J., Koovakkat, S. K., Liang, A., Mohan, R., Phillips, G. B., Seto, M., Shaw, K. J., Xu, W., Zhao, Z., Light, D. R., & Morrissey, M. M. (1999). Crystallographic analysis of potent and selective factor Xa inhibitors complexed to bovine trypsin. *Acta Crystallogr., D* *55*, 1395–1404.
- Wolfson, H. J. & Rigoutsos, I. (1997). Geometric hashing: An overview. *IEEE Comput. Sci. Eng.* *4*, 10–21.
- Wu, H., Dong, A., Zeng, H., Loppnau, P., Weigelt, J., Sundstrom, M., Arrowsmith, C. H., Edwards, A. M., Bochkarev, A., & Plotnikov, A. N. (2006). The crystal structure of human FtsJ homolog 2 (*E. coli*) protein in complex with AdoMet. PDB entry 2NYU.
- Xiao, T., Takagi, J., Collier, B. S., Wang, J. H., & Springer, T. A. (2004). Structural basis for allostery in integrins and binding to fibrinogen-mimetic therapeutics. *Nature* *432*, 59–67.
- Xie, L. & Bourne, P. E. (2008). Detecting evolutionary relationships across existing fold space, using sequence order-independent profile-profile alignments. *Proc. Natl. Acad. Sci. USA* *105*, 5441–5446.

Acknowledgments

The authors thank Kengo Kinoshita, Motonori Ota and Hiroyuki Toh for helpful discussion, and Daron M. Standley for critically reading the manuscript. This work was supported by a grant-in-aid from Institute for Bioinformatics Research and Development, Japan Science and Technology Agency (JST). H. N. was supported by Grant-in-Aid for Scientific Research (B) No. 20370061 from Japan Society for the Promotion of Science (JSPS).